2015 American Control Conference
Palmer House Hilton
July 1-3, 2015. Chicago, IL, USA

Self-contained, Ultrasonic Sensor-based Mobility Generation for Differential Drive UGVs

Ahmad A. Masoud, Mohanad Ahmed, Ali Al-Shaikhi,
Electrical Engineering, King Fahad University of Petroleum & Minerals, Dhahran, Saudi Arabia
masoud@kfupm.edu.sa, mohanadahmed@kfupm.edu.sa, shaikhi@kfupm.edu.sa,

Abstract: This paper suggests a self-contained, mobility system for velocity controlled, differential drive robots in unknown cluttered environments. The system tackles the use of ultrasonic sensing at the servo-level to generate motion. It can, in real-time, convert the raw measurements from the onboard ultrasonic sensors to a control signal that safely propels the robot to its target. The structure uses a safety-based, subjective representation of the environment to synthesize the control signal. This significantly relaxes the burden of having to accurately localize the components of the environment. Moreover, the structure can decouple the computational burden from the size of the environment representation, hence enabling real-time servo-level navigation. The structure is implemented and thoroughly tested on the X80 mobile robot platform using only one out of the six ultrasonic sensors the robot has (the front sensor). The test consistently demonstrated that the robot can safely reach its target, from the first attempt, along a well-behaved trajectory using well-behaved control signals.

I. Introduction

Mobility is a core capability any autonomous agent must have in order to function [1]. Mobility itself is a composite activity that emerges from the interaction of basis activity modules. One of these modules is concerned with the acquisition of data about the environment [2]. This data is mainly collected by onboard sensors. However, *a priori* available data may be supplied by an external agent. The data is processed and structured by a representation module [3,4]. The function of this module is to generate a form which the agent may use to execute the intended task. This form is called an environment representation or a context map. The localization module [5] functions to make the position of the agent on the map corresponds to its true location in the environment. Guidance provides the agents with the sequence of reference tasks it's supposed to execute in order to reach the target [6,7]. As for the control module [8,9], its job is to instruct the agent's actuators of motion on what to do so that a reference task is realized.

Individually, each one of the above modules has been extensively studied with many techniques suggested for implementation. The criteria used to assess performance are usually module-centered and do not take the networked nature of mobility into consideration. Despite the intensive work on each module, many issues relating to how they function are still considered to be an open area of research [10]. There is a growing concern that a modularized view of mobility leads to an overly complicated system with shaky performance. The trend is growing to develop theoretical frameworks that jointly examine the construction of more than one of these modules. Examples of this are: simultaneous localization and mapping [11], direct guidance from sensory (observation) space [12,13], joint guidance and control [14]. To the best of these authors' knowledge, a theoretical framework that jointly tackles all the modules needed for providing an autonomous agent with mobility does not exist. Putting together a complete mobility system is mainly dependant on the experience of the designer [15,16]. Physical experiments seem to be the only way to verify the performance of such systems.

In this paper we suggest a self-contained mobility system for a velocity controlled differential drive robot. The data acquired from the robot's onboard ultrasonic sensors is converted in real-time to a control signal capable of propelling the robot along a safe path to its target from the first attempt. Although ultrasonic sensors are both affordable and practical, their utilization is challenging both in terms of real-time operation (i.e direct coupling to the servo loop) and operation in an unstructured environment. Converting the signal from the ultrasonic sensors to a reliable map of the environment is both complex and computationally intensive [17, 18]. Even if fast enough processors are present, the available techniques for reliably converting the ultrasonic sensor data into a map of the environment assume that the obstacles of the environment are orthogonal to each other [19]. This assumption is highly unlikely to hold in an unstructured environment. Another challenge has to do with the size of the map grid needed to represent a realistic environment. Each dimension of the grid is in hundreds of pixels (even thousands). Sensor-based operation requires that the environment representation be incrementally built and the corresponding navigation policy be continuously adjusted. It is obvious that brute force re-computation from scratch is out of the question. It should be possible to locally & incrementally update the representation and the corresponding navigation policy based on the data the sensors make available to the agent at a certain instant in time. Localization is also a big challenge facing the construction of a reliable mobility module. Even involved procedures such as SLAM [11] do face problems when operating in feature-scarce domains. It is also highly desirable that the system does not engage an exploration phase before it starts driving the agent to the target. Rather, in time sensitive missions, the mobility system should immediately start steering the robot to the target collecting only the necessary and sufficient data, given the situation the robot is facing.

In addressing the above requirements, the suggested mobility structure avails itself, among other things, from two concepts. The first is: subjectively-constructed environment maps. Instead of using objective spatial maps (geometrical or topological) that accurately reflect the physical structure of the environment, subjective maps require only that the robot be at a safe location [20] if its current location on the map is marked safe. It also requires that the robot be at the target if

its location on the map is marked as a target location. This arrangement significantly relaxes the localization requirement and confines strict localization to the target only. The second concept is harmonic potential field-based (HPF) motion planning [21,22]. While HPF planners do possess a considerable number of properties that are important to the construction of an integrated mobility system [26], a novel feature of the HPF approach is used to enable the coupling of the ultrasonic sensors directly to the servo-loop. That is: if HPFs are disturbed by introducing local constraints, the effect of the newly introduced constrains is effectively localized to the vicinity of the change. This property enables decoupling of the computational burden from the size of the map.

This paper is organized as follows: section 2 contains the problem statement. Section 3 describes the mobility components while in section 4 these components are interconnected to yield the mobility structure. Experimental results are in section 5 and conclusions are in section 6.

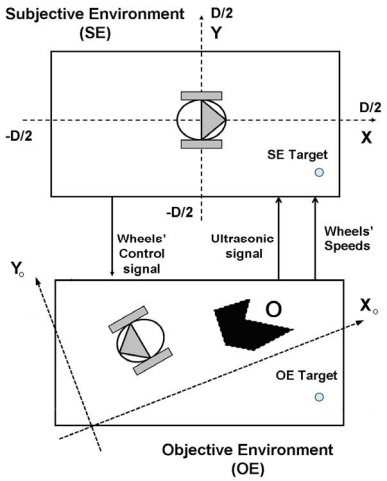

Figure-1: Objective and subjective environments of the robot

II. Setting & Problem Statement

The work in this paper views the representation as the subjective environment (SE) of the robot that need not strictly reflect the geometry of the real environment (objective environment, OE). SE has only two links to OE (figure-1):

1- if the robot is at a safe place in SE then it is at a safe place in OE

2- if the robot reaches the target in SE then it reaches the target in OE.

A square domain of operation (Γ) of width D is assumed. It is called the perimeter of operation. A Cartesian coordinate system (x,y) is embedded in Γ so that the origin is at the center of the domain. Initially, the center of the robot is assumed to lie at the environment center (x=0,y=0). It is also assumed to be initially oriented along the x-axis (θ=0). A target point (x_T,y_T) is selected in SE so that when the robot is located at (x_T,y_T) in SE it is also located at (xo_T,yo_T) in OE.

The motion equations of a velocity controlled differential drive robot (figure-2) are:

$$\begin{bmatrix}\dot{x}\\ \dot{y}\\ \dot{\theta}\end{bmatrix}=\begin{bmatrix}\cos(\theta) & 0\\ \sin(\theta) & 0\\ 0 & 1\end{bmatrix}\begin{bmatrix}v\\ \omega\end{bmatrix},\quad \begin{bmatrix}v\\ \omega\end{bmatrix}=\begin{bmatrix}\frac{r}{2} & \frac{r}{2}\\ \frac{r}{W} & \frac{-r}{W}\end{bmatrix}\begin{bmatrix}\omega_R\\ \omega_L\end{bmatrix},\quad \begin{bmatrix}\omega_R\\ \omega_L\end{bmatrix}=\begin{bmatrix}\frac{1}{r} & \frac{W}{2\cdot r}\\ \frac{1}{r} & \frac{-W}{2\cdot r}\end{bmatrix}\begin{bmatrix}v\\ \omega\end{bmatrix}\quad (1)$$

Where v is the tangential velocity of the robot, ω is its angular speed, ω_R, ω_L are the angular speeds of the right and left wheels, r is the radius of the wheels and W is the separation between the two wheels.

Minimal sensing is used; the mobility structure relies only on one ultrasonic sensor to generate the control signals for the robot's wheels. The main lobe of the sensor is aligned along the principal axis of the robot. The sensor produces the continuous output S(t). Ideally, S(t) provides a measurement of the distances between the sensor and the closest obstacle in OE that lies along the principal axis of the robot. A zero value of S(t) is an indicator that either no obstacle exist along the principal axis or the obstacle is out of sensor range. In both cases, if S(t)=0 it is assumed that no obstacle exist.

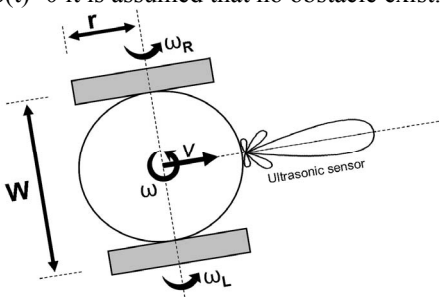

Figure-2: Velocity controlled differential drive robot

Using only the wheels' speeds ($\Omega=[\omega_R \quad \omega_L]^T$), the target location in SE ($X_T=[x_T \quad y_T]^T$) and readings from the sensor (S(t)), a control velocity signal ($\Omega c=[\omega c_R \quad \omega c_L]^T$) is synthesized

$$\Omega c = F(\Omega, X_T, S(t))$$

Such that $\lim_{t\to\infty} X \to X_T$ and (2)

$$R(t)\cap O \equiv \phi \quad \forall t.$$

where R(t) and O are the regions occupied by the robot and obstacles respectively in OE.

III. The Components of the Mobility Structure

In this section, the modules used to construct a mobility system with the above capabilities are described.

It is widely believed that the signal from an ultrasonic sensor needs to undergo extensive processing in order to be usable for robot navigation. This paper demonstrates that the raw output from only one ultrasonic sensor aligned along the principal axis of the robot is highly likely to provide enough information to navigate an autonomous mobile robot in a challenging unknown environment.

III.1 Safety map construction:

The context in which the robot is operating is recorded at a resolution Δ using an NxN matrix (figure-3) DSE(i,j) (Δ=D/N). If DSE(i,j) is marked by 1, the location indexed by i & j is considered unsafe. If it is marked by 0, the location is considered possibly safe. DSE is constructed as follows: first the matrix is initialized

$$DSE(1,i)=DSE(N,i)=DSE(i,1)=DSE(i,N)=1 \quad i=1,..N,$$
$$DSE(i,j)=0 \quad i=2,..N-1,\ j=2,..N-1\ . \quad (3)$$

At a certain instant in time, given a robot's pose (x,y,θ), DSE is populated as follows:

$$Io=\left[\frac{x+(S+R)\cdot\cos(\theta+\delta)}{\Delta}\right],\quad Jo=\left[\frac{y+(S+R)\cdot\sin(\theta+\delta)}{\Delta}\right] \qquad (4)$$

$$DSE(Io+m,Jo+n)=1 \quad n=-Im,..Im,\ m=-Im,..Im$$
$$N>Io+m>1,\ N>Jo+n>1$$

where R is the distance from the center of the robot to where the sensor is located, Im is a nonnegative integer constant used as a safety margin surrounding the sensed obstacle location, [X] is the rounding integer function of the real number X and 1>>δ>0. It ought to be noticed that sensing errors caused by spurious reflections do not endanger robot's safety. This is due to the fact that these errors will cause a safe location to be marked as unsafe. Since the sensor is aligned along the direction of motion, it is not possible for the robot to move into an unsafe location. Therefore the sensor-map pair does provide a safe and dynamic representation for the robot. The worst case sensing artifacts and localization error could lead to is partial loss of safe and usable space.

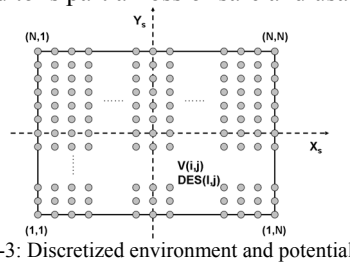

Figure-3: Discretized environment and potential field

III.2 Localization

Deadreckoning is used for localization. Advanced deadreckoning techniques [23], even precise optical deadreckoning [24], do exist. However, here, for the purpose of demonstrating the robustness of the structure, we use a basic form of deadreckoning that directly compute the robot's pose from its wheels' speeds. We don't even use Kalman filtering to obtain a refined estimate of the robot's pose:

$$\begin{bmatrix}\nu\\ \omega\end{bmatrix}=\begin{bmatrix}\frac{r}{2} & \frac{r}{2}\\ \frac{r}{W} & \frac{-r}{W}\end{bmatrix}\begin{bmatrix}\omega_R\\ \omega_L\end{bmatrix},$$

$$\nu x=\nu\cdot\cos(\theta)\ ,\ \nu y=\nu\cdot\sin(\theta) \qquad (5)$$

$$x(t+\Delta T)=x(t)+\Delta T\cdot\nu\cdot x(t)\ ,$$

$$y(t+\Delta T)=y(t)+\Delta T\cdot\nu y(t)$$

$$\theta(t+\Delta T)=\theta(t)+\Delta T\cdot\omega(t) \quad x(0)=0,\ y(0)=0,\ \theta(0)=0$$

III.3 Guidance:

A guidance module functions to convert mission data (environment representation, goal and constraints on operation) into the sequence of subtasks it needs to carry-out in order for the goal to be reached in the desired manner. There are a large number of techniques one may choose from in order to generate guidance activities. The harmonic potential approach to planning and guidance seems to fit well the task at hand. The approach amasses a lot of critical properties needed for successful integration in a mobility system [26]. The approach is provably-correct, it can operate in a model-based or sensor-based modes [25], it can process vague information [22], it can enforce, in a provably-correct manner, a variety of constraints on motion [21] and it yields analytic trajectories guaranteeing the construction of a provably-correct control. A basic setting of the harmonic approach is:

$$\text{Solve} \qquad \nabla^2 V(x,y)\equiv 0 \qquad x,y\in\Pi$$
$$\text{Subject to:}\quad V(x_T,y_T)=0,\quad V(x,y)=1 \quad x,y\in\partial\Pi \qquad (6)$$

Motion is safely guided to the target using the gradient dynamical system:

$$\begin{bmatrix}\dot{x}\\ \dot{y}\end{bmatrix}=-\begin{bmatrix}\partial V/\partial x\\ \partial V/\partial y\end{bmatrix}=\begin{bmatrix}Gx\\ Gy\end{bmatrix} \qquad (7)$$

where Π is the workspace of the robot and $\partial\Pi$ is the boundary of Π.

Executing guidance in the servo loop is made possible by a previously unutilized property of the harmonic approach. The property has to do with the ability of the harmonic approach to localize the disturbance caused by introducing a new environment component to the vicinity of that component. Let V be a harmonic function constructed from the set $\partial\Pi$. Also, let Vp be a harmonic potential constructed from the set $\partial\Pi\cup P$, where P is a newly introduced point obstacle. If B is a spherical region with center P and radius ε, then one can show that an ε maybe found such that

$$|V-Vp|<\delta \qquad \forall x,y\notin B. \qquad (8)$$

where δ is an arbitrarily small positive number. In other words, there is no need to recomputed V outside B. The following example illustrates this property. Figure-4 shows the guidance field from a harmonic potential obtained for an environment that consists of a square obstacle representing the robot's perimeter and an internal point obstacle. The finite difference method was used to solve for the potential. The field is computed fully on the 40x40 grid and partially by updating the obstacle-free field with the field computed on a 15x15 window around the point obstacle. As can be seen, the fields are almost identical. More importantly, the navigational properties of the harmonic potential are preserved.

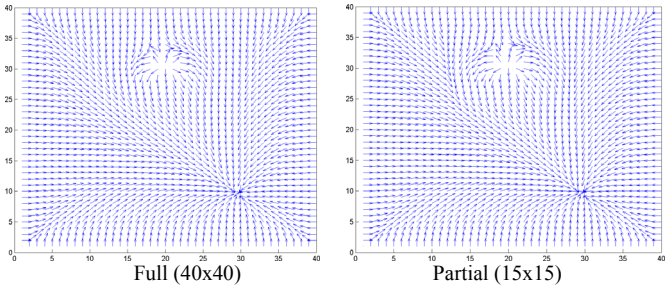
Full (40x40) Partial (15x15)
Figure-4: full & partial guidance field computation

III.4 Control

Generating the navigation control signal is based on the work in [27]. The approach is provably-correct. The aim of the control signal is to synchronize the velocity of the robot with the guidance velocity from the negative gradient of the harmonic potential (figure-5). The result is a provably-correct navigation control signal that can be made to inherit all the properties of the guidance signal. In the following, the

navigation control for a velocity controlled differential drive robot is realized using a hardware friendly form.

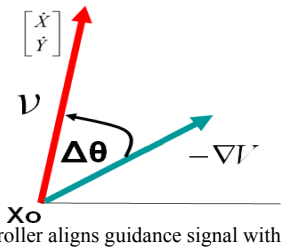

Figure-5: Controller aligns guidance signal with robot's velocity

First the sine and cosine of the angle between the velocity of the robot and the guidance velocity ($\Delta\theta$) are computed along with the straight line distance to the target (dst).

$$\eta_d = \cos(\Delta\theta) = \frac{Gx \cdot vx + Gy \cdot vy}{\sqrt{vx^2 + vy^2}}, \qquad (9)$$

$$\eta_c = \sin(\Delta\theta) = \frac{Gx \cdot vy - Gy \cdot vx}{\sqrt{vx^2 + vy^2}}$$

$$dst = \sqrt{(x - x_T)^2 + (y - y_T)^2}$$

The desired tangential vc and angular ωc speeds of the robot are computed, where vd and ωd are the maximum tangential and angular speeds the robot should assume. The desired tangential speed profile as a function of $\Delta\theta$ for $\omega d = 1$ is shown in figure-6

$$vc = vd \cdot \begin{bmatrix} 1 & dst > Rc \\ \frac{dst}{Rc} & dst \le Rc \end{bmatrix}, \qquad (10)$$

$$\omega c = \omega d \cdot \begin{bmatrix} \eta_c & \eta_d > 0 \\ +1 & \eta_c > 0 \; and \; \eta_d < 0 \\ -1 & \eta_c < 0 \; and \; \eta_d < 0 \end{bmatrix}$$

were Rc is an arbitrary small positive number. The velocity control signals that are to be applied to the robot's wheels are computed using equation-11. The overall structure of the navigation controller is shown in figure-7.

$$\begin{bmatrix} \omega C_R \\ \omega C_L \end{bmatrix} = \frac{1}{r} \cdot \begin{bmatrix} 1 & \frac{W}{2} \\ 1 & -\frac{W}{2} \end{bmatrix} \begin{bmatrix} vc \\ \omega c \end{bmatrix} \qquad (11)$$

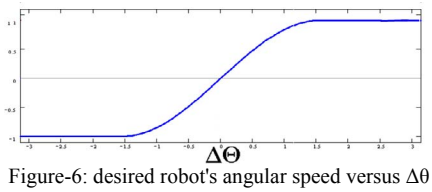

Figure-6: desired robot's angular speed versus Δθ

IV. The Mobility Structure:

In this section the modules discussed above are integrated to yield the mobility structure. The structure is described using the flowchart in figure-8.

First, the structure needs to be initialized by specifying the subjective coordinates which data is recorded with respect to. The perimeter (D) of SE is also supplied along with the target in SE which has to be the image of the target in OE. The guidance field is then globally computed given the initial information available. The wheels' speeds of the robot and the ultrasonic sensor measurements are recorded. If no obstacles are within the sensor range of the robot (S=0), the pre-computed guidance information is used. If an obstacle facing the robot is detected, it is mapped into the subjective environment of the robot. The guidance field is then locally recomputed around the added environment component and the modified guidance information is obtained. Using the robot's wheels' speeds the pose of the robot in SE is updated. This information is combined with the guidance signal to compute the control signals (wheels' speeds control signals). The control signals are applied to the robot and the speeds of the robot's wheels are monitored. The procedure for constructing the navigation control is provably-correct. In other words, if there is a path to the target, the robot will not stop until the target is reached. If the robot stops short of reaching its target, then the cause of the problem has to be the partial field computation stage. Since motion did halt, computing the guidance field in real-time is no longer important. Therefore, the full field computation stage is invoked to correct this problem.

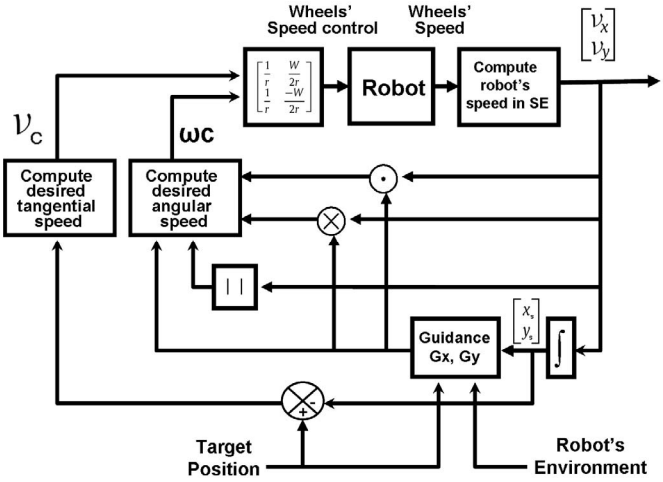

Figure-7: The suggested, hardware-friendly controller

V. Experimental results

The structure, as a whole and individually as components, was extensively examined using simulation. However, only experimental results are reported in this paper. An inexpensive platform (X80 UGV) is used to experimentally validate the structure. Only sensor-based experiments are reported; model-based experiments are not reported. The obstacles of the environment are constructed from cable drums. The structure of cable drums creates considerable scattering of the ultrasonic signal. Also the base being wider than the middle support provides a good test of the safety of the generated trajectories.

The structure's ability to move the X80 to a target point under zero initial information about the environment using only one front ultrasonic sensor was tested for many obstacles' configurations. All runs produced satisfactory results (figure-9)

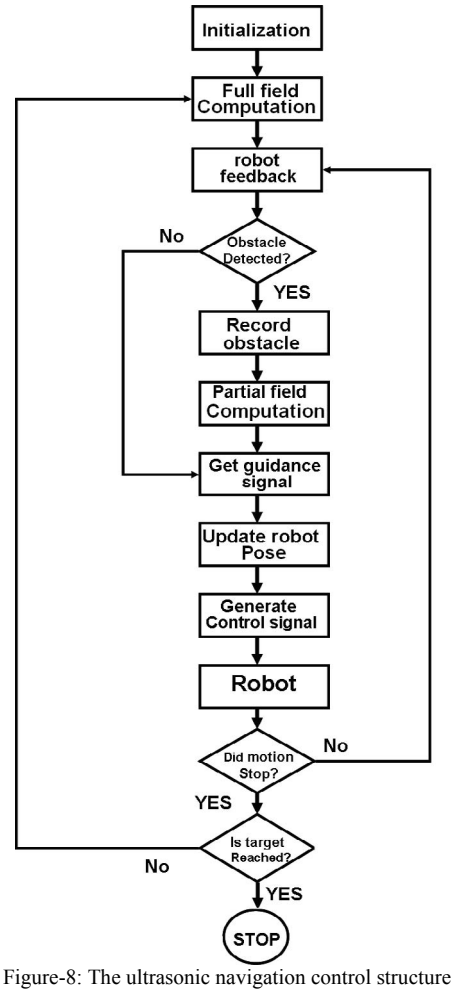

Figure-8: The ultrasonic navigation control structure

Figure-9: trials of X80 moving to a target in an unknown environment

In the following, a detailed example is provided for the proposed control structure. Photos of the environment along with snapshots of the path taken by the robot are shown in figure-10. The control structure managed to drive the robot to the target zone using only the raw measurements recorded by the front ultrasonic sensor.

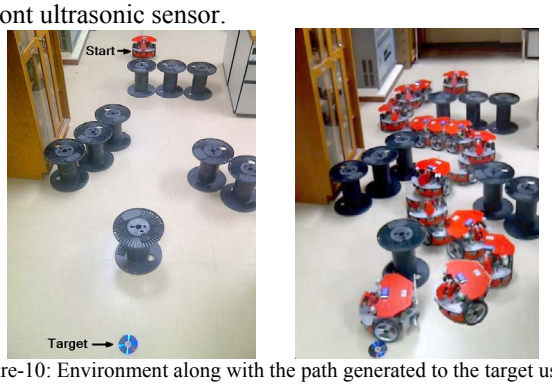

Figure-10: Environment along with the path generated to the target using only the front ultrasonic sensor.

Figure-11 shows the trajectory of the robot superimposed on the safety map (SE) constructed from the raw ultrasonic sensor data and the trajectory superimposed on the actual map of the environment (OE). As can be seen, the recorded subjective map significantly deviates from the objective map of the environment. It is interesting to notice that the path corresponds nicely to the geometry of the OE, even keeps a good safety margin from the obstacle.

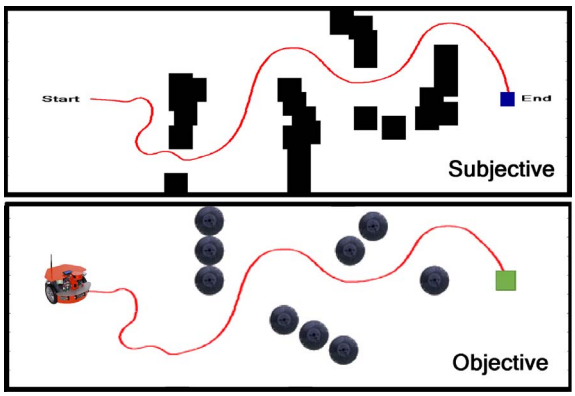

Figure-11: Robot's trajectory corresponds well to the objective map of the environment

The signal from the sensor is shown in figure-12. Although the signal is highly unstructured, rapidly fluctuating and has severe discontinuities, the control signals (figure-13) are continuous and well-behaved.. The orientation of the robot as a function of time is shown in figure-14. Notice the smoothness of the angular profile and the low curvature.

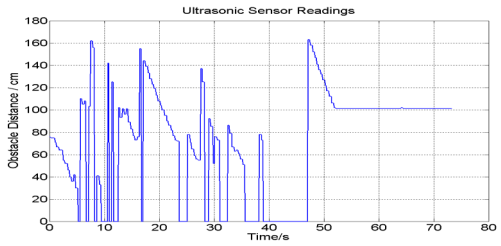

Figure-12: Signal from the X80 ultrasonic sensor

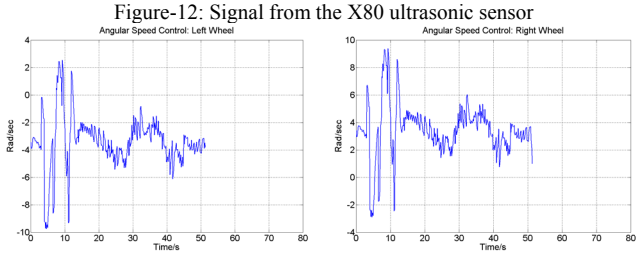

Figure-13: The X80 wheels control signals

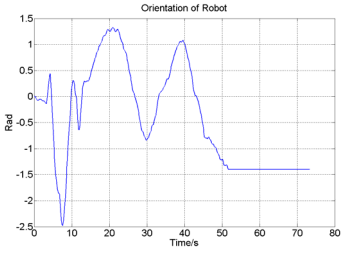

Figure-14: Orientation of the X80 body

VI. Conclusions

In [28] Khatib demonstrated that potential fields may be used to construct an efficient and time critical method for generating mobility at the servo level. Khatib explicitly mentioned in the paper that the approach is not meant for planning. It is only meant to provide fast robot reaction to avoid collision with obstacles. This paper provides a proof of principle that the potential field approach is not only suitable for motion planning at the servo-level of a robot, it can also provide a provably-correct, ultrasonic sensor-based servo-level navigation control signal. The paper also demonstrates the centrality of the guidance module (motion planner) to the overall mobility structure. As can be seen, no processing has been done on the ultrasonic signal. Also, naive deadreckoning is used. As for the control structure, it only attempts to make the navigation control the image of the guidance signal. With all these shortcomings, the robot projected satisfactory and repeatable performance. The work in this paper provides a strong reason to re-examine the belief that accurate, spatial mapping of the environment is a perquisite to satisfactorily navigate an unstructured environment. Experimental results show that proceeding towards the target under zero *a priori* information while collecting only the data needed to guarantee safety can produce trajectories with good differential, state and integral characteristics. The work also demonstrates that it is possible to carry-out reliable navigation using impoverished sensing and cheap hardware that is prone to actuator saturation and noise with limited computational capacities.

The authors gratefully acknowledge the assistance of king Fahad University of Petroleum and Minerals.

References

[1] D. Gage, "UGV HISTORY 101: A Brief History of Unmanned Ground Vehicle (UGV) Development Efforts", Special Issue on Unmanned Ground Vehicles, Unmanned Systems Magazine, Summer 1995, volume 13, number 3, pp. 1-9

[2] M. Kulich, P. Stopan, L. Preucil, "Knowledge Acquisition for Mobile Robot Environment Mapping", Database and Expert Systems Applications, Lecture Notes in Computer Science Volume 1677, 1999, pp 123-134

[3] D. Wooden, "A Guide to Vision-Based Map Building", IEEE Robotics and automation magazine, June 2006, pp. 94-98

[4] C. Castejo, B. Boada, D. Blanco, L. Moreno, "Traversable Region Modeling for Outdoor Navigation", Journal of Intelligent and Robotic Systems (2005) 43: 175–216

[5] L. Feng, J. Borenstein, and B. Everett, 1994, " Where am I? Sensors and Methods for Autonomous Mobile Robot Localization." Technical Report, The University of Michigan UM-MEAM-94-21, December 1994.

[6] C. Goerzen; Z. Kong; B. Mettler, "A survey of motion planning algorithms from the perspective of autonomous UAV guidance", Journal of Intelligent and Robotic Systems: Theory and Applications.2010;57(1-4):65-100

[7] N. Rao, S. Kareti, W. Shi, S. Iyengar, "Robot Navigation in Unknown Terrains: Introductory Survey of Non-Heuristic Algorithms", Oak Ridge National Laboratory, Tech. Rep. ORNL/TM-12410, July 1993.

[8] G. Campion, B. d'Andrea-Novel, G. Bastin, Controllability and state feedback stabilizability of non holonomic mechanical systems, in: Advanced Robot Control, in: Lecture Notes in Control and Information Sciences, vol. 162, 1991, pp. 106–124

[9] G. Campion, G. Bastin, B. D'Andrea-Novel, Structural properties and classification of kinematic and dynamic models of wheeled mobile robots, IEEE Transactions on Robotics and Automation 12 (1) (1996) 47–62.

[10] M. Salichs and L. Moreno, "Navigation of mobile robots: open questions", Robotica, Volume 18, Issue 03, May 2000, pp 227 - 234

[11] G. Grisetti, R. Kümmerle, C. Stachniss, and W. Burgard, "A Tutorial on Graph-Base SLAM", IEEE Intelligent Transportation Systems IEEE Magazine, Winter 2010, pp. 31-43,

[12] A. Censi, A. Nilsson, R. Murray, "Motion planning in observations space with learned diffeomorphism models", Proceedings of the IEEE International Conference on Robotics and Automation (ICRA), 2860–2867. Karlsruhe, Germany, 5 2013

[13] A. Censi, "Bootstrapping Vehicles: a Formal Approach to Unsupervised Sensorimotor Learning Based on Invariance", Ph.D, California Institute of Technology Pasadena, California, 2013.

[14] A. Masoud, "A Harmonic Potential Approach For Simultaneous Planning And Control Of A Generic UAV Platform", From The Issue "Special Volume On Unmanned Aircraft Systems" Of Journal Of Intelligent & Robotic Systems: Volume 65, Issue 1 (2012), Page 153-173

[15] S. Thrun, T. Mitchell, "Lifelong Robot Learning", The Biology and Technology of Intelligent Autonomous Agents NATO ASI Series Volume 144, 1995, pp 165-196,

[16] A. Stentz, M. Hebert, "A Complete Navigation System for Goal Acquisition in Unknown Environments", Autonomous Robots, 1995, Volume 2, Issue 2, pp 127-145

[17] A. Elfes, "Occupancy Grids: A probabilistic framework for robot perception and navigation", Ph.D, Electrical Engineering, CMU, 1989

[18] B. Min, D. Cho, S. Lee, Y. Park, "Sonar mapping of a mobile robot considering position uncertainty", Robotics and Computer-Integrated Manufacturing, Volume 13, Issue 1, March 1997, Pages 41–49

[19] K. Chong, L. Kleeman, "Mobile Robot Map Building from an Advanced Sonar Array and Accurate Odometry", Robotics and Automation, 1997. Proceedings., 1997 IEEE International Conference on (Volume:2), April 20-25, pp. 1700-1705, 1997

[20] A. Murarka, "Building Safety Maps using Vision for Safe Local Mobile Robot Navigation", ph.D., The University of Texas at Austin August 2009

[21] S. Masoud, A. Masoud, " Motion Planning in the Presence of Directional and Obstacle Avoidance Constraints Using Nonlinear Anisotropic, Harmonic Potential Fields: A Physical Metaphor", IEEE Transactions on Systems, Man, & Cybernetics, Part A: systems and humans, Vol 32, No. 6, November 2002, pp. 705-723.

[22] A. Masoud, "Motion Planning With Gamma-Harmonic Potential Fields", Aerospace and Electronic Systems, IEEE Transactions on 48 (4), 2012, pp. 2786 - 2801

[23] L. Banta, "Advanced Dead-reckoning Navigation for Mobile Robots", Ph.D, Mechanical Engineering, Georgia institute of technology, 1987

[24] D. Sekimori, F. Miyazaki, "Precise Dead-Reckoning for Mobile Robots Using Multiple Optical Sensors", Informatics in Control, Automation and Robotics II, pp. 145-151, 2007, Springer

[25] A. Masoud, Samer A. Masoud, "Evolutionary Action Maps for Navigating a Robot in an Unknown, Multidimensional, Stationary Environment, Part II: Implementation and Results", the 1997 IEEE International Conference on Robotics and Automation, April 21-27, Albuquerque, New Mexico, USA, pp. 2090-2096.

[26] R. Gupta, A Masoud, M. Chow, "A Delay-Tolerant, Potential Field-Based, Network Implementation Of An Integrated Navigation System", The IEEE Transactions On Industrial Electronics, Vol. 57, No.2, February 2010, PP. 769-783

[27] A. Masoud, "A Harmonic Potetnial Field Approach For Joint Planning & Control Of A Rigid, Seprable, Nonholonomic, Mobile Robot", Robotics And Autonomous Systems, Volume 61, Issue 6, June 2013, Pages 593–615.

[28] O. Khatib, "Real-Time Obstacle Avoidance for Manipulators and Mobile Robots", The International Journal of Robotics Research March 1986 vol. 5 no. 1 90-98.